frontiers | Frontiers in Marine Science

TYPE Original Research
PUBLISHED 13 June 2025
DOI 10.3389/fmars.2025.1599456

OPEN ACCESS

EDITED BY
Josipa Ferri,
University of Split, Croatia

REVIEWED BY
Catalina Perales-Raya,
Centro Oceanográfico de Canarias (IEO-CSIC), Spain
Zdravko Ikica,
University of Montenegro, Montenegro

*CORRESPONDENCE
Bilin Liu
bl-liu@shou.edu.cn
Hu Zhang
ahu80@163.com

RECEIVED 25 March 2025
ACCEPTED 16 May 2025
PUBLISHED 13 June 2025

CITATION
Liu B, Ou Y, Zhou M, Zhang H, Xiao Y, Zu K, Zhu C and Hu H (2025) Study on the age and growth characteristics of *Sepia esculenta* in the East coast of China based on beak microstructure. *Front. Mar. Sci.* 12:1599456. doi: 10.3389/fmars.2025.1599456

Study on the age and growth characteristics of *Sepia esculenta* in the East coast of China based on beak microstructure

Bilin Liu[1,2,3,4]*, Yuzhe Ou[1], Minhua Zhou[1], Hu Zhang[5]*, Yueyue Xiao[5], Kaiwei Zu[5], Chaowen Zhu[5] and Haisheng Hu[5]

[1]College of Marine Living Resources and Management, Shanghai Ocean University, Shanghai, China, [2]Key Laboratory of Sustainable Exploitation of Oceanic Fisheries Resources, Ministry of Education, Shanghai, China, [3]Key Laboratory of Oceanic Fisheries Exploration, Ministry of Agriculture and Rural Affairs, Shanghai, China, [4]National Distant-water Fisheries Engineering Research Center, Shanghai Ocean University, Shanghai, China, [5]Jiangsu Marine Fisheries Research Institute, Nantong, Jiangsu, China

This study investigates the daily age and growth characteristics of *Sepia esculenta* along the East coast of China, aiming to provide essential data for population dynamics and sustainable fisheries management. A total of 360 specimens were collected from September to November 2021. Among these, 178 individuals (81 females and 97 males) were successfully aged by analyzing growth increments in the sagittal section of the upper beak rostrum (RSS) using beak microstructure analysis. The mantle length (ML) of *S. esculenta* ranged from 55 to 201 mm and body weight (BW) from 30 to 667 g, with no significant sex differences. Age estimates ranged from 59 to 152 days, averaging 106.44 ± 17.35 days for females and 103.86 ± 19.70 days for males. The ML-age relationship fitted a linear growth model, while BW-age relationships followed an exponential model for females and a power function model for males. Growth rate analysis showed varied growth trajectories with age, with the highest absolute growth rate (AGR) of ML observed at 120–150 days for females (1.23 mm/d) and at 60–90 days for males (1.93 mm/d). These findings provide crucial insights into the growth patterns and population dynamics of *S. esculenta* in the East coast of China, supporting resource assessment and sustainable management efforts.

KEYWORDS

***Sepia esculenta*, beak microstructure, age, growth, the coastal waters of**

1 Introduction

Sepia esculenta belongs to Cephalopoda, Sepioidea, Sepiidae, Sepia. This species is a warm-temperate cephalopod that is widely distributed along the coastal regions of the western Pacific, particularly in the nearshore waters of countries such as China, South Korea, Japan, and the Philippines. It primarily inhabits benthic environments at depths ranging from 10 to 100 meters, with a preference for muddy or sandy seabed (Dong, 1991; Qi, 1998). The *S. esculenta* displays notable migratory behavior, typically dwelling in deeper waters during the winter and migrating to coastal regions to spawn in the spring and summer. Its main breeding period occurs from April to July each year. Similar to other cephalopod species, *S. esculenta* has a short life cycle and rapid growth rate, typically living for only one year and dying after spawning (Ikeda et al., 2009; Boyle and Rodhouse, 2005). *S. esculenta* is an important target for fisheries in China's nearshore waters due to its significant economic value (Guo et al., 2022). Its flesh is highly valued for its delicate taste and high protein content, while its internal shell is renowned for its medicinal properties (Al-Rawe et al., 2024). The *S. esculenta* is a carnivorous species, with its diet changing as it matures. In its juvenile and early life stages, it primarily preys on crustaceans (mainly shrimp and crabs), amphipods, and small fish. As adults, they expand their diet to include larger prey such as shrimp, crab, and juvenile cuttlefish, occasionally engaging in cannibalism (Zhao et al., 2024; Hao et al., 2007). Furthermore, the *S. esculenta* serves as a vital food source for numerous marine predators, including seabirds, large fish, and marine mammals, playing a key role in energy transfer and material cycling within marine ecosystems (Wei et al., 2005).

In previous studies on the age and growth of cephalopods, statoliths have typically been the preferred material for age determination. Growth increments and morphological features in statoliths have revealed information on the growth patterns, growth variations, seasonal fluctuations, and life history traits of different cephalopod species (Chen et al., 2011), providing valuable scientific data for fisheries resource assessment and management. However, differences in the morphology and formation of growth increments exist among species, and not all cephalopod statoliths exhibit clear microstructural growth patterns. In some species, the uneven distribution of pigment deposits in the statolith microstructure hinders the clear observation of growth increments and the core (Perales-Raya et al., 1994; Fang et al., 2022), complicating the verification of the "one increment per day" hypothesis for growth marks (Arkhipkin, 2005). Beak growth increments and marks can be used to estimate the age of cephalopods (Castanhari and Tomás, 2012; Liu et al., 2015; Chen et al., 2022), particularly in cases where statoliths are difficult to obtain or unsuitable for analysis. The beak, a crucial feeding organ in cephalopods, is one of the most important hard tissue structures. It is morphologically stable, resistant to corrosion, and exhibits some degree of synchronicity with the animal's growth, thus recording abundant life history information (Armelloni et al., 2020; Xavier et al., 2023), similar to statolith growth patterns. The accumulation of chitin in the beak is comparable to the deposition of calcium carbonate in the statoliths, both reflecting rhythmic activity patterns in *Octopus vulgaris* that are influenced by light-dark cycles (Hernández-López et al., 2001). Compared to statoliths, cephalopod beaks are larger, more durable, easier to preserve, and simpler to measure (e.g. Liu et al., 2015). The daily periodicity of growth increments in the beaks has been validated in several species within the squid (Liu et al., 2016, 2020; Lu et al., 2022. Oosthuizen (2003) conducted an experiment on *O. vulgaris* using tetracycline and successfully marked five individuals. The study revealed uneven visibility of tetracycline marks in the beak. Perales-Raya et al. (2014a) conducted a study on wild *O. vulgaris* maintained and marked in aquaria, and provided evidence for the daily deposition of growth increments in both the lateral wall surface (LWS) and the rostral sagittal section (RSS) of the chitinous beak. Guerra-Marrero et al. (2023a) carried out a study on the rearing of *Sepia officinalis* hatchlings, quantifying the number of growth increments in the beak and comparing them with the days post-hatching. Their results confirmed the "one increment per day" deposition pattern, indicating that each growth increment corresponds to a single day. Agus et al. (2024) validated the use of the beak microstructure for age determination in *S. officinalis* by cross-verifying the daily growth increments observed in both statolith and beak microstructures. Their findings further support the suitability of the beak as a reliable hard tissue for age estimation in members of the order Sepioidea. Beak growth rates are influenced by various factors such as food availability, temperature, and reproductive cycles (Arkhipkin, 2005). By analyzing beak growth, growth curves for cephalopods under different environmental conditions can be constructed, providing insights into their life cycle and growth dynamics (Perales-Raya et al., 2014a). The morphology and wear patterns of the cephalopod beak can also reflect the type of prey and feeding strategies, and the analysis of beak damage can offer insights into the predatory behavior of their predators and their position within the food chain (Xavier et al., 2023). Furthermore, distinct morphological differences in beaks across cephalopod species make them valuable tools in cephalopod taxonomy and species identification, particularly in stomach content analysis, such as examining digestive residues found in large fish and whales (Miserez et al., 2010; Harvey et al., 2014).

Recent studies on the age and growth of the *S. esculenta* in China's nearshore waters are scarce. This study, based on samples collected from the East coast of China between September and November 2021, aims to analyze the basic biological characteristics of *S. esculenta*. We analysis the growth increments of the *S. esculenta* 's beak, establish growth models for daily age, mantle length (ML), and body weight (BW), and explore the age-growth characteristics, growth rate, and growth patterns of this species. The age and growth data of *S. esculenta* in the East coast of China baseline biological information essential for stock assessments by helping to estimate growth rates, age structure, and recruitment patterns. These insights can improve predictions of population dynamics and trends, and support the development of more effective and sustainable fishery management strategies.

2 Materials and methods

2.1 Sampling

From September to November 2021, random sampling of *S. esculenta* was conducted off the East coast of China using a fishing vessel. Following each sampling event, the collected samples were immediately frozen for preservation. A total of 360 *S. esculenta* specimens were captured. After freezing, the samples were transported to the laboratory for fishery biology experiments and dissection. Complete beaks were extracted for age determination through analysis of their microstructure, yielding 178 valid age data points: 97 males and 81 females. The success rate of age acquisition was 49.44%. The sampling location is shown in Figure 1.

2.2 Biological measurements

After thawing, the ML and BW of *S. esculenta* were measured with an accuracy of 1 mm and 1 g, respectively. The sex and sexual maturity stages were visually assessed and classified according to standard morphological characteristics of the gonads (Hu et al., 2016; Chen et al., 2013). Based on these criteria, specimens were divided into five maturity stages: immature (Stages I and II), mature

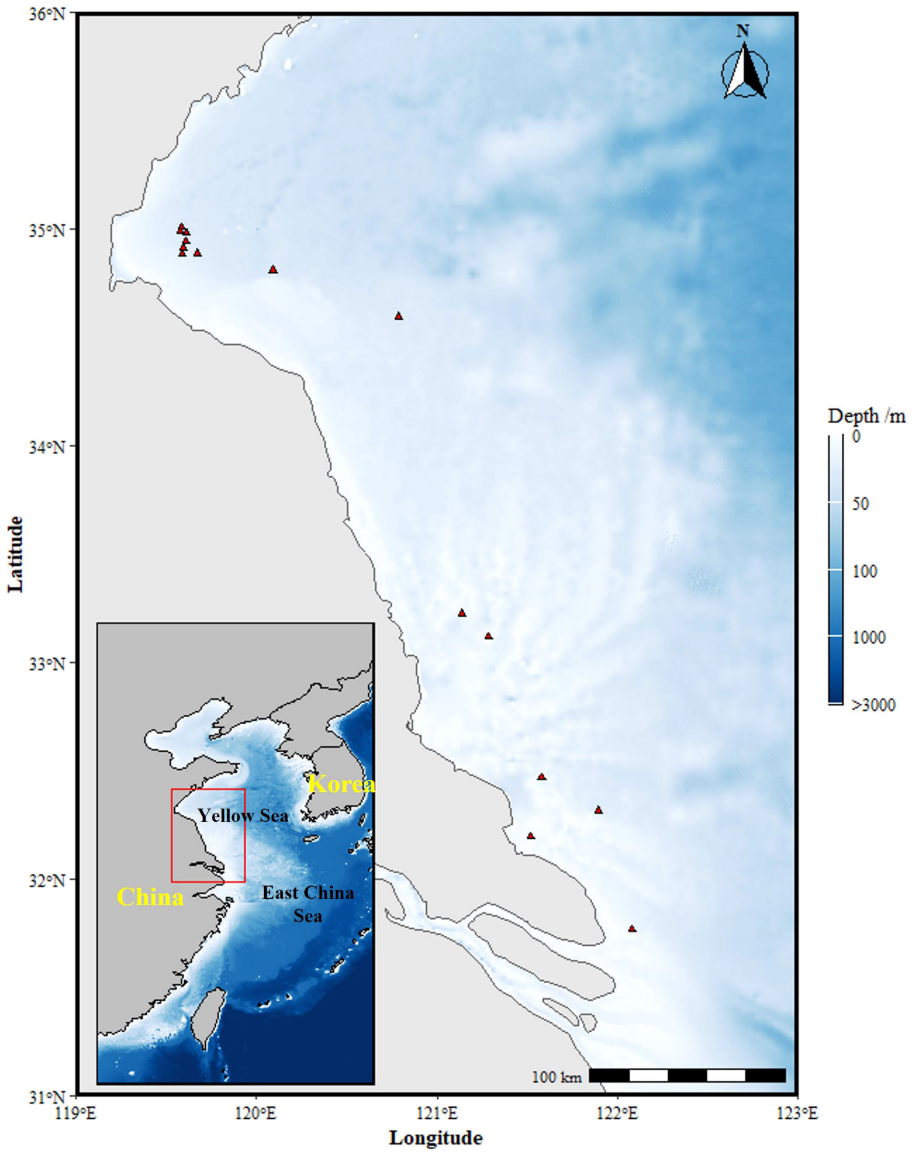

FIGURE 1
Sampling stations of survey along the East coast of China.

(Stages III, IV, and V). The extracted hard tissues of the specimens were cleaned of surface impurities using ultrapure water and preserved for further analysis. The beaks were placed in centrifuge tubes and stored in a 75% ethanol solution at room temperature.

2.3 Beak processing and age reading

After grinding, distinct incremental structures can be observed. The preparation of upper beak sections follows a standardized procedure, including cutting, embedding, grinding, and polishing (Liu et al., 2015). To obtain sagittal sections, the beak is first cut from the anterior portion along the midline of the hood to the posterior edge using a precision cutting tool, ensuring that the cutting plane remains parallel to the RSS. The RSS is then excised smoothly and placed into an embedding mold. The orientation of the sample is carefully adjusted, and a 1:1 volume ratio of curing agent to cold embedding resin is applied for fixation. The embedded samples are left to harden in a cool, undisturbed environment for 24–48 hours. After hardening, the samples grinded on both sides sequentially with waterproof sandpapers of grits 80, 600, 1200, 2000, 2400, and 4000. During grinding, the sample was repeatedly examined under a microscope until the growth increments were fully and clearly visible. Afterward, a polishing solution containing 0.05 μm alumina powder was applied for polishing. Finally, the prepared beak sections were observed under an Olympus optical microscope using diascopy illumination (transmitted light from below) to enhance transparency and structural detail. Simultaneous images were captured from different regions of the beak sections using a charge-coupled device (CCD) system. These images were later stitched together using Photoshop 24.0 to create a composite image of the same sample. This method was used to accurately read the growth increments in the beak (Chen et al., 2022; Yatsu et al., 1997). The growth increments on beak are symmetrically distributed. When the issue of tip erosion in the RSS, counting the growth increments along the lateral wall inner surfaces can help reduce the potential underestimation of age. Two independent researchers read the growth increments of each beak sample, and the difference between their respective age readings must be less than 10% of the mean value for the data to be considered valid (Chen et al., 2011; Hu et al., 2016).

2.4 Data analysis

A t-test was conducted to evaluate the differences in ML and BW between male and female *S. esculenta*. Additionally, an analysis of covariance (ANCOVA) was performed to examine whether significant differences existed in age-ML and age-BW between sexes. In this study, six growth models were used to fit the growth relationship of *S. esculenta* (Arkhipkin and Laptikhovsky, 2000; Brunetti and Ivanovic, 1997). The equations for each model are as follows:

Linear model:

$$L_t = a + bt$$

Exponential model:

$$L_t = a \times e^{bt}$$

Power function model:

$$L_t = a \times t^b$$

Logistic growth model:

$$L_t = \frac{\mathrm{a}}{1 + \mathrm{Exp}(-\mathrm{b}(\mathrm{t}-\mathrm{c}))}$$

Von Bertalanffy growth model:

$$L_t = \mathrm{a} \times (1 - \mathrm{Exp}(-\mathrm{b} \times (\mathrm{t}-\mathrm{c}))$$

Gompertz growth model:

$$L_t = \mathrm{a} \times \mathrm{Exp}(\mathrm{b} \times (1 - \mathrm{Exp}(-\mathrm{c} \times \mathrm{t})))$$

Where ?$_?$ represents the ML (or BW) at age t (in mm, g); ? is the age; and *a*, *b*, and *c* are the parameters.

The best-fitting model was selected based on the Akaike Information Criterion (AIC). The model with the lowest AIC value was considered the optimal model (Chen et al., 2011).

The absolute growth rate (AGR) and instantaneous relative growth rate (IRGR) were used to analyze the growth rate variations in ML and BW of *S. esculenta*. The growth rates were calculated using the following equations (Liu et al., 2013).

$$AGR = \frac{Q_2 - Q_1}{t_2 - t_1}$$

$$IRGR = \ln(X_2) - \ln\frac{(X_1)}{t_{2-}t_1}$$

Where Q_2 represents the mean ML (mm) or BW (g) at age ?$_2$; Q_1 represents the mean ML (mm) or BW (g) at age t_1; AGR is expressed in mm/day or g/day, while IRGR is expressed in %/day.

3 Result

3.1 ML and BW composition

The sex ratio of the 178 collected S. esculenta specimens (81 females and 97 males) was 1:1.2 (female: male), indicating a slightly higher proportion of males in the sampled population. The ML of all specimens ranged from 55 mm to 201 mm, and individuals were categorized into ML groups at 30 mm intervals. For females, the ML ranged from 81 mm to 196 mm, with an average ML of 115.71 ± 35.78 mm. The dominant ML group was 91—180 mm, accounting for 90.12% of the total female samples. For males, the ML ranged from 55 mm to 201 mm, with an average ML of 113.53 ± 38.00 mm. The dominant ML group was 91—180 mm, comprising 89.69% of the total male samples (Figure 2). The results of the t-test (F=1.497,

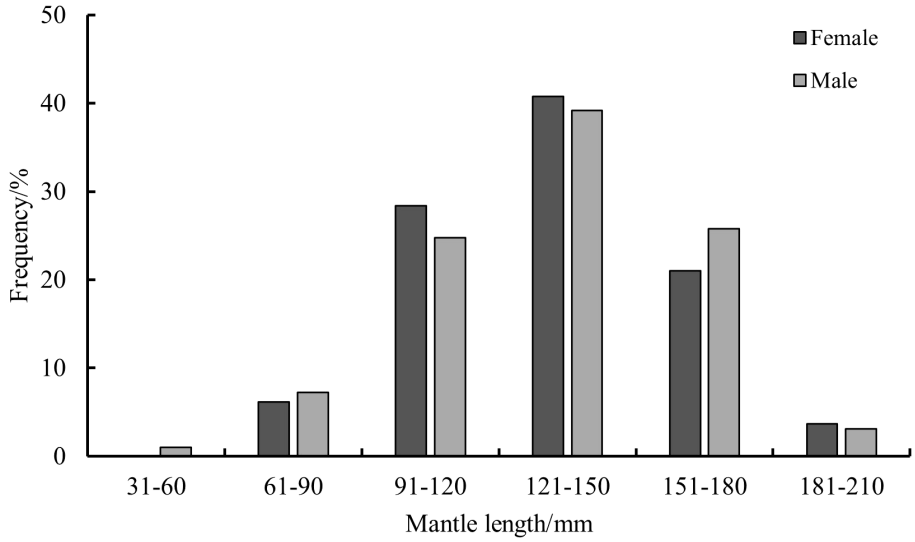

FIGURE 2
Distribution of ML of *S.esculenta*.

t=0.149>0.05) indicated that there was no significant difference in ML between males and females.

The BW of *S. esculenta* specimens ranged from 30 g to 667 g, and individuals were categorized into BW groups at 100 g intervals. For females, BW ranged from 55 g to 667 g, with an average BW of 190.66 ± 153.05 g. The dominant BW group was 101—400 g, accounting for 77.78% of the total female samples. For males, BW ranged from 30 g to 623 g, with an average BW of 185.01 ± 142.63 g. The dominant BW group was 101—500 g, comprising 87.63% of the total male samples (Figure 3). The results of the t-test (F=0.001, t=0.501>0.05) indicated that there was no significant difference in BW between males and females.

3.2 Beak microstructure

The microstructure of the RSS of the upper beak in *S. esculenta* primarily consists of two distinct regions: internal of hood and crest (Figure 4a). Hood is the part of the rostrum attached by the rostral edge to the lateral wall, which lies outside or lateral to the lateral wall. Crest is the joint between the top of the two lateral walls (Clarke et al., 1986). A clear internal rostral axis separates the hood and crest regions within the RSS microstructure (Raya and Hernández-González, 1998). The growth increments in the hood and crest regions intersect at the internal rostral axis, forming a characteristic "a left-pointing chevron"(Figure 4b). These growth increments differ in width,

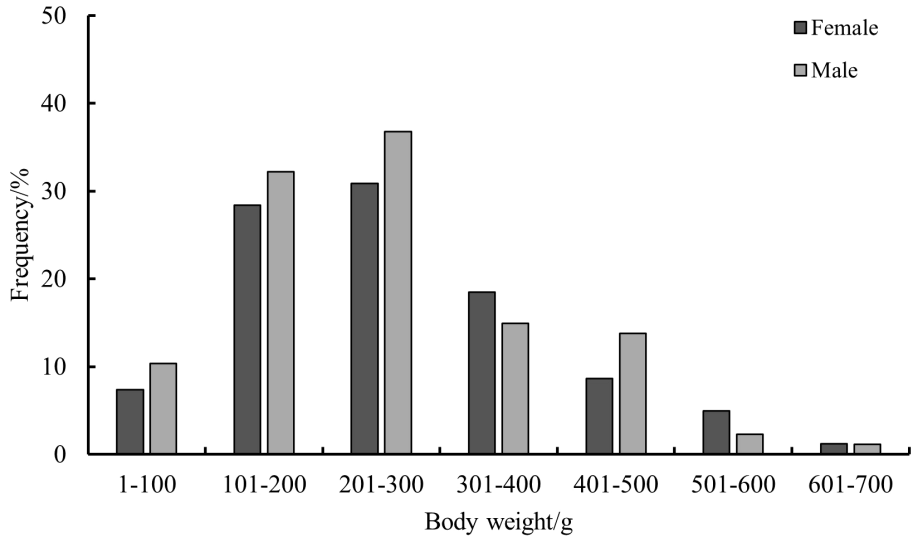

FIGURE 3
Distribution of BW of *S.esculenta*.

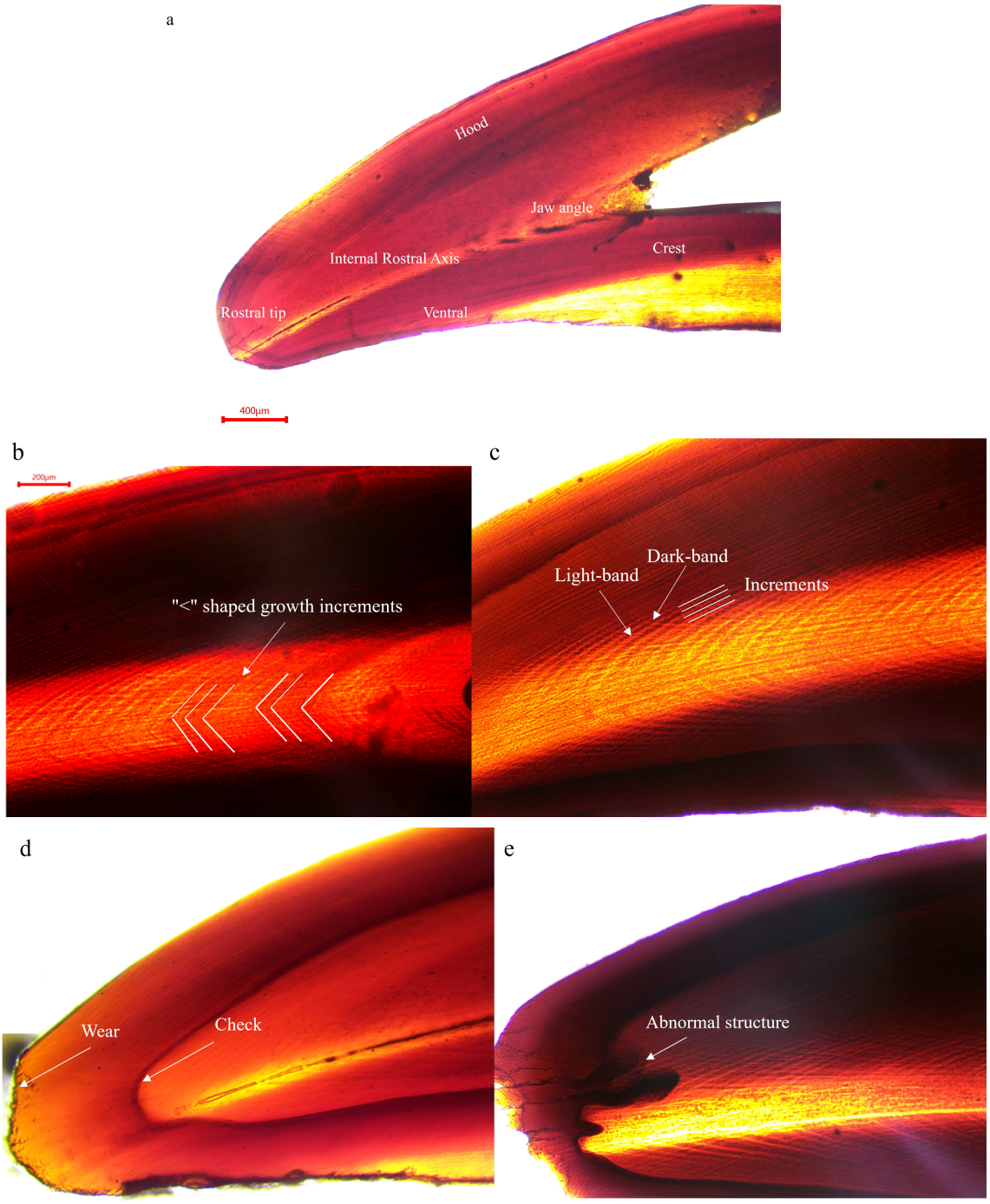

FIGURE 4
(a) the upper beak microstructure of *S. esculenta*; **(b)** the shape of growth increments; **(c)** light and dark bands and growth increments; **(d, e)** the check increments in the hood region and abnormal structure.

number, and spacing, with the hood region exhibiting more distinct and well-defined growth increments. Its growth increments appear as alternating light and dark bands that grow periodically, exhibiting a pattern of daily deposition (Figure 4c). Additionally, wear and notches are observed at the apex of some beak microstructures, and the RSS of the upper beak is more prone to the formation of check increments and irregular growth patterns (Figures 4d, e). The check increments were characterized by light bands that appeared lighter than the surrounding light increments, and dark bands that were darker than the typical dark increments. These features suggest potential influences from environmental factors or individual biological conditions on beak growth and microstructural variations.

3.3 Age composition and sexual maturity

The age range of the beak of *S. esculenta* from 59 to 152 days, with age groups divided at intervals of 30 days. Females exhibit an age range of 72 to 149 days, with an average age of females is 106.44 ± 17.35 days. The dominant age group being 81—140 days, comprising 83.51% of the total sample. The youngest individual at 72 days, having a ML of 82 mm and a weight of 55 g, and the oldest individual at 149 days, with the ML of 196 mm and the weight of 667 g. For males, the age range is from 59 to 152 days, with an average age of 103.86 ± 19.70 days. The dominant age group for males is 81—140 days, comprising 88.89% of the total sample. The youngest male is 59 days, with a ML of 55 mm and a weight of 30 g, while the oldest male is 152 days, with a ML of 201 mm and a weight of 623 g (Figure 5).

In this study, the majority of *S. esculenta* samples were in the immature stage, and the proportion of mature individuals decreased as the maturity stage increased. Among female samples, 27.16% were in maturity stage I, and 66.67% were in stage II; stages III and IV accounted for only 4.94% and 1.23%, respectively. For male samples, 37.11% were in maturity stage I, and 60.82% were in stage II; stage III represented only 2.06%, with no individuals in stage IV (Figure 6).

3.5 Growth model

The results of ANCOVA indicated that there is a significant gender difference in the growth of ML and age of *S. esculenta* ($F=0.082$, $P=0.00 < 0.05$). Therefore, in subsequent analyses of the growth relationship, separate analyses were conducted for the relationship between age and ML in female and male individuals. Through equation fitting, maximum likelihood optimization, and AIC comparison, the best growth models for both female and male *S. esculenta* age and ML were represented by linear functions (Table 1, Figure 7a). The relationships are as follows:

The growth models of age-ML for females:

$$L = 1.3786t - 13.957 (R^2 = 0.92,\ N = 81)$$

The growth models of age-ML for males:

$$L = 1.3829t - 12.031 (R^2 = 0.91,\ N = 97)$$

The results of ANCOVA indicated significant gender differences in the relationship between age and BW of *S. esculenta* ($F=0.143$, $P=0.00 < 0.05$). Therefore, separate analyses were conducted for the relationship between age and BW in female and male individuals. Through equation fitting, maximum likelihood optimization, and AIC comparison, the best growth model for the relationship between weight and age in female *S. esculenta* was represented by an exponential function, while the best growth model for male individuals was described by a power function (Table 1, Figure 7b). The relationships are as follows:

The growth models of age-BW for females:

$$L = 15.626e0.0253t\ (R^2 = 0.71,\ N = 81)$$

The growth models of age-BW for males:

$$L = 0.0013tx2.6078\ (R^2 = 0.81,\ N = 97)$$

3.6 Growth rate

The AGR of ML in female *S. esculenta* ranged from 1.12 to 1.23 mm/d, while the IRGR varied between 0.62% and 11.14%. The highest AGR (1.23 mm/d) was observed at an age of 120–150 days, during which the IRGR showed a declining trend. In males, the AGR of ML ranged from 1.13 to 1.93 mm/d, with an IRGR between

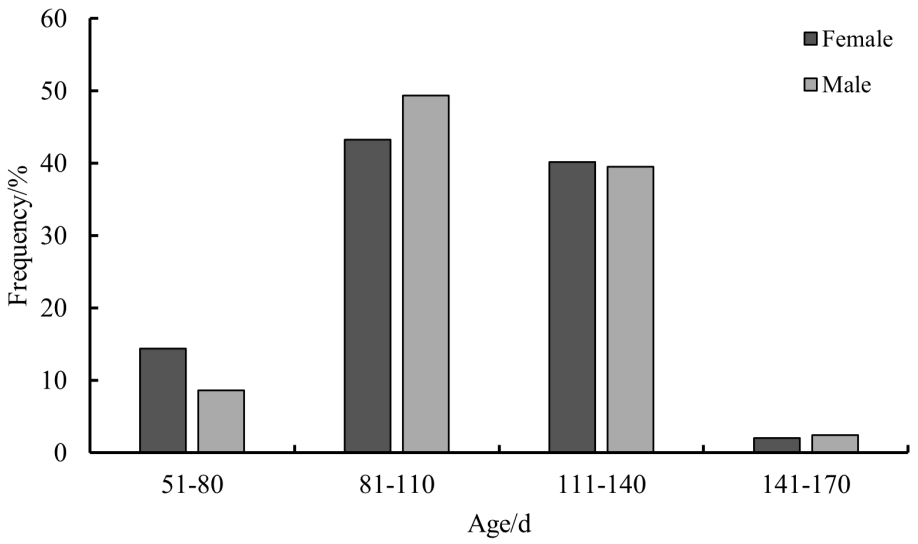

FIGURE 5
Age composition of *S. esculenta*.

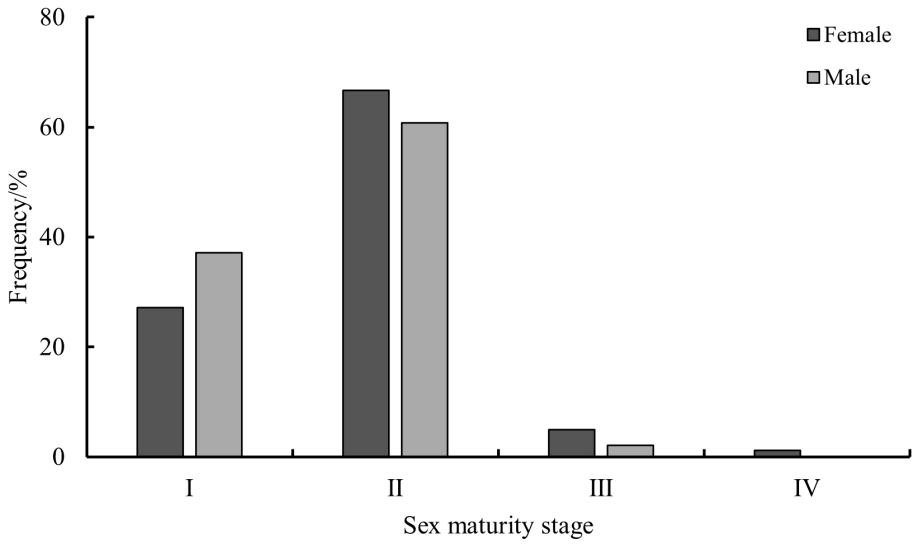

FIGURE 6
Sexual maturity composition of *S. esculenta*.

0.75% and 2.66%. The highest AGR (1.93 mm/d) was recorded at an age of 60–90 days, while the IRGR exhibited a decreasing trend (Figures 8a, b).

The AGR of female *S. esculenta* BW ranged from 2.44 to 10.12 g/d, and the IRGR ranged from 1.58% to 2.56%. The highest AGR (10.12 g/d) occurred at an age of 150–180 days, with an overall increasing trend. The maximum IRGR (2.56%) was observed at an age of 120–150 days, with the overall IRGR showing a decreasing trend. For males, the AGR of BW ranged from 3.86 to 9.33 g/d, with the highest AGR (9.33 g/d) recorded at an age of 150–180 days, showing an overall increasing trend. The maximum IRGR (6.37%) occurred at an age of 60–90 days, with the IRGR showing a declining trend overall (Figures 8c, d).

4 Discussion

4.1 ML and BW composition

The measurement and analysis of biological indices serve as the foundation for cephalopod fisheries biology research, as fundamental biological indices often vary among individuals and populations. ML and BW are two critical biological parameters in cephalopods, providing a direct representation of individual size and growth status. In this study, the ML of *S. esculenta* ranged primarily from 91—180 mm, while BW was mainly distributed between 101—300 g. These values were higher than those reported by Fei (2020) for *S. esculenta* collected during the same season in 2017 in the coastal waters of Shandong, which may be attributed to interannual variations in the marine environment. Previous research by Qu et al. (2021) adequately suggested that cuttlefish have a short life cycle and rapid growth, making their growth characteristics highly susceptible to environmental factors such as seawater temperature and ocean currents. Consequently, variations in growth and development may occur across different habitats or between years. The results of this study indicate that there are no significant differences in ML and BW between male and female *S. esculenta* the East coast of China . This finding is consistent with the results of Xue et al. (2024), based on S. esculenta samples collected annually from September to the following March between 2017 and 2021 in the central East China Sea. This may be due to similar survival strategies during the early growth stages of cephalopods, preventing the emergence of pronounced differences (Dan et al., 2025). Furthermore, the average ML and BW of female *S. esculenta*

TABLE 1 AIC values of growth models for *S. esculenta*.

Sex	Model	Linear		Power		Exponential		Logistic		Von Bertalanffy		Gompertz	
		R^2	AIC	R^2	AIC	R^2	AIC	R^2	AIC	R^2	AIC	R^2	AIC
Female	Age-ML	**0.9215**	**515.35**	0.9136	514.71	0.9050	527.15	0.8353	615.25	0.8386	612.58	0.8405	611.02
	Age-BW	0.7084	1121.85	0.7124	1112.98	**0.7144**	**1104.62**	0.7052	1120.69	0.6318	1154.61	0.7117	1117.63
Male	Age-ML	**0.9191**	**554.43**	0.9165	554.74	0.8965	575.21	0.8178	663.66	0.8213	661.7	0.8223	660.35
	Age-BW	0.7644	1088.98	**0.8120**	**1081.55**	0.7883	1099.65	0.7664	1090.97	0.7109	1117.99	0.7640	1117.63

Bold text indicates the best model.

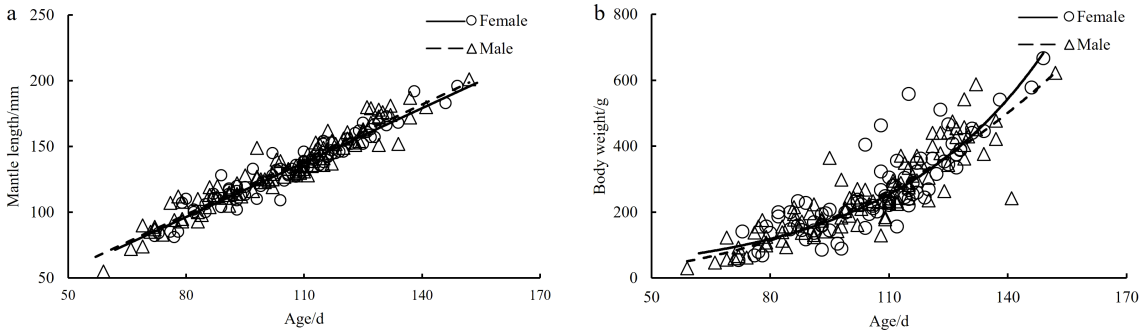

FIGURE 7
(a, b) The growth models of age-ML and age-BW for *S. esculenta*.

were greater than those of males, aligning with the findings of Wei et al. (2005), who also observed similar trends in their study on the biological characteristics of *S. esculenta* sampled from Lanshan, Rizhao, between June 2002 and October 2003. This discrepancy may be explained by the growth transition in females occurring at the onset of sexual maturity development (Stage II), whereas in males, this transition begins only when the gonads reach a more advanced developmental stage (Stage III) (Xue et al., 2024). Differences in juvenile squid growth among generations are not only closely related to variations in spawning and hatching times across years but are also influenced by fluctuations in recruitment abundance, resource availability, and prey dynamics (Niu et al., 2017). Similar observations of females being larger than males have been reported in other cephalopods, including *Sepiella inermis* (Jahan and Mahmud, 2025), African cuttlefish *Sepia bertheloti* (Guerra-Marrero et al., 2023b), *Ommastrephes bartramii* (Fang et al., 2016), *Sthenoteuthis oualaniensis* (Ou et al., 2022), and *Dosidicus gigas* (Hu et al., 2016). This phenomenon may be attributed to the continuous growth of female reproductive organs, such as the ovary and oviducal gland, as the individual matures, resulting in a more pronounced and rapid increase in female body size compared to males. During different growth stages of cephalopods, energy allocation varies, and distinct energy distribution patterns are observed between sexes even at the same developmental stage (Chen et al., 2020; Sieiro et al., 2020; Pascual et al., 2020).

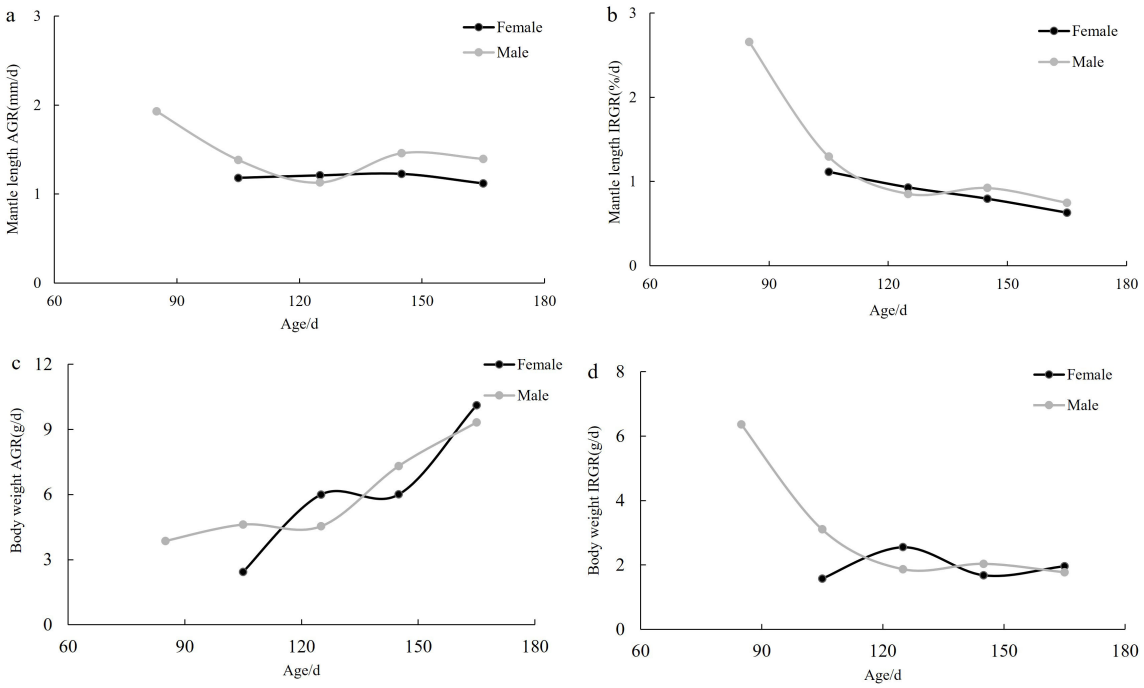

FIGURE 8
(a–d) The relationship between the growth rates of *S. esculenta* (ML and BW) and age (AGR, absolute growth rate; IRGR, instantaneous relative growth rate).

4.2 Beak Microstructure

The cephalopod beak is primarily composed of proteins and chitin fibers, exhibiting a relatively stable shape and high rigidity (Clarke, 1962; Miserez et al., 2007). The daily growth increments of *S. esculenta* are primarily located in the RSS of the upper beak (Fang et al., 2022). In this study, the microstructure of the upper beak of *S. esculenta* was analyzed, and the periodicity of growth increments was observed to determine age. These findings are in agreement with those of Fang et al. (2022), who reported similar beak microstructural patterns in cephalopods such as *D. gigas* (Hu et al., 2016) and *Octopus*. (Perales-Raya, 2014a). The study identified regularly spaced growth increments in the RSS of the upper beak, manifested as alternating dark and light bands, which likely reflect endogenous biological rhythms, potentially linked to diel or seasonal variations in feeding or locomotor activity (Cobb et al., 1995; Raya and Hernández-González, 1998). The hood region of *S. esculenta* exhibited deeper pigment deposition, while the crest region showed relatively lighter pigment deposition, making the growth increments more distinguishable. However, the spacing between increments in the hood region was wider than in the crest region, allowing for more accurate age determination. This pattern has also been observed in other cephalopod species (Chen et al., 2022; Hu et al., 2016). The variation in increment spacing within the same region may be related to different life history stages; early-stage individuals exhibit rapid growth with wider increment spacing, whereas later-stage individuals experience slower growth with narrower spacing (Perales-Raya et al., 2010). Based on beak microstructure analysis, Perales-Raya et al. (2020) reported a decreasing trend in increment width in Architeuthis dux, from the young ages (16.4 µm of average for first 30 increments) to the oldest ages (10.2 µm for the latest 30 increments).

Additionally, habitat temperature may influence the spacing of growth increments. Studies have shown that *D. gigas* from warmer waters exhibits larger increments compared to individuals from colder waters (Liu et al., 2015). In this study, distinct check increments were also observed, which may provide evidence of specific life events or environmental changes during the growth of *S. esculenta*, including shifts in environmental conditions, critical life history transitions, and predator attacks (Arkhipkin, 2005; Perales-Raya et al., 2014b). Furthermore, wear and structural modifications at the anterior portion of the beak are likely caused by mechanical damage sustained during prey capture and processing. Similar patterns of wear and structural adaptation have been reported in the beak microstructures of other cephalopods (Lu et al., 2022; Chen et al., 2022).

4.3 Age composition and sexual maturity

Previous studies have shown that *S. esculenta* exhibits rapid generational turnover and a short lifespan, it is an annual species (Natsukari and Tashiro, 1991). It typically spawns from June to August, undergoes growth and development from September to February of the following year, and reaches sexual maturity between March and May (Wei et al., 2005). In this study, the collected specimens had an average age of 104 days, with the oldest individual recorded at 152 days (approximately five months), further confirming the summer spawning pattern of *S. esculenta*. The age of *S. esculenta* is closely linked to its growth and developmental stages. In this study, the samples were collected from September to November, a period during which offspring individuals of *S. esculenta* undergo rapid growth. This timing may explain why the majority of the samples were in an immature stage. Previous research on *S. esculenta* in the central East China Sea from September to March of the following year indicated seasonal differences in sexual maturity. Specifically, individuals collected from September to November were predominantly in sexual maturity development stages I and II (Xue et al., 2024), which is consistent with the results of this study. This suggests that *S. esculenta* typically attains sexual maturity in winter and spring, whereas in autumn, a significant proportion remains immature. Additionally, a small number of sexually mature individuals were identified in this study. It was observed that female *S. esculenta* reached sexual maturity at a smaller ML compared to males, indicating possible precocious maturation in the female population. In recent years, advancements in fishing technologies, increased catch yields, and changes in the marine environment have exerted growing pressure on *S. esculenta* populations (Hao et al., 2007; Fang et al., 2022). The observed early maturation trend may represent an adaptive reproductive strategy in response to high fishing pressure and habitat changes, aimed at increasing population persistence (Xue et al., 2024). Therefore, to ensure the sustainable management of *S. esculenta* resources, it is essential to explore regional stock enhancement strategies, maintain a balance between supply and demand within the habitat, and protect the ecological environment. Developing scientifically informed strategies for the quality and quantity of released juveniles in enhancement programs is crucial for the long-term conservation of this species.

4.4 Growth model

This study utilized six growth models to construct age-ML and age-BW growth models for *S. esculenta*, aiming to describe its growth characteristics. The analysis of *S. esculenta* specimens collected from September to November revealed that the growth model for the relationship age-ML is best represented by a linear function, which aligns with the growth models of *S. esculenta* in the East China Sea described by Fang et al. (2022). The general growth pattern in cephalopods is characterized by differing growth rates at various life stages (Forsythe and Van Heukelem, 1987; Boyle and Rodhouse, 2008). Typically, the growth rate is faster during the juvenile stage, while it slows down during the adult stage. Overall, growth trends are often best described by nonlinear models such as the Logistic, exponential, or logarithmic functions (Guo et al., 2023). For example, Lu et al. (2022) based on the beak of *S. oualaniensis* in the northwest Indian Ocean found that the linear growth model for the autumn population was the best fit for the

relationship between age and ML, while the power function was the best model for the spring population to describe the age-ML relationship. Chen et al. (2022) also found that exponential functions were the best to describe the growth of age-ML and age-BW for *S. oualaniensis* in the South China Sea. Additionally, Li et al. (2021) based on statolith found that the growth of age-ML in spring-spawning *Uroteuthis edulis* was best fit by the Logistic, while the summer-spawning population's growth was best fit by the von Bertalanffy. Sex is also a key factor influencing growth in cephalopods. Our study demonstrated that the growth model for female *S. esculenta* age-BW was best described by an exponential function, while the male growth model was best described by a power function. Guerra-Marrero et al. (2023b) found that the growth model for males of the African cuttlefish *S. bertheloti* was best fitted using the von Bertalanffy model, while the female growth model was best described by an exponential function. For the entire population (both males and females), an exponential model best represented growth. Hu et al. (2016) found that the relationship age-BW of the *D. gigas* in the Peruvian exclusive economic zone is best fitted by an exponential growth model. Cephalopod growth and age are influenced by multiple factors, and growth equations suitable for different sexes, populations, and geographic locations often differ (Arkhipkin, 1997; Jackson, 2004). Liu et al. (2013) suggested that nonlinear models can reflect the overall growth trend throughout the species' life history, while linear models are more suitable for capturing growth characteristics during specific stages of an individual's development. Therefore, using multiple models for fitting in the construction of cephalopod growth models can improve the accuracy of model fitting.

4.5 Growth rate

The results of this study did not detect significant differences in growth rates between male and female *S. esculenta*. The maximum AGR of female ML occurred 120–150 days, reaching 1.23 mm/d, while the maximum AGR of male ML occurred 60–90 days, reaching 1.93 mm/d. However, this result may have some bias, as the number of male samples at 60–90 days was relatively small. Additionally, a peak in the growth rate of male ML was also observed between 120–150 days, with a value of 1.46 mm/d. Both the AGR of the female and male BW showed an upward trend, with a decline in AGR followed by a rapid increase between 120–150 days. This phenomenon could be attributed to *S. esculenta* changing its habitat and prey types, thus obtaining more food to meet its growth requirements. Oceanographic characteristics significantly influence the distribution of cephalopod larvae (Boyle and Rodhouse, 2005). Cephalopod larvae have limited migratory abilities and initially feed along the continental shelf edge. As their swimming and predation abilities improve, they can migrate from the shelf to deeper ocean waters, resulting in a dietary shift (Sajikumar et al., 2018). Furthermore, after 120 days, the AGR of male ML was higher than that of females, while the growth of female BW showed a certain lag compared to males, with a higher growth rate. This may be related to their development stage. Most of the *S. esculenta* samples collected in this study were in the immature and over-mature stages, suggesting that female individuals likely allocate more energy to gonad development during growth, which is reflected in the continuous increase in BW. In contrast, male individuals tend to invest energy in body growth during the maturation process. This phenomenon has also been observed in other cephalopods' age-growth studies (Arkhipkin, 1997; Boyle and Rodhouse, 2005; Dawe and Beck, 1997). The sampling period in this study was from September to November, during the growth stage, with relatively young individuals and low sexual maturity. Therefore, future studies on the age and growth of *S. esculenta* should include long-term sampling programs to assess the potential spatiotemporal variability in age and growth.

5 Conclusion

This study analyzes the microstructure of the beak of *S. esculenta* collected from the East coast of China, revealing the age-growth characteristics of this species. Assuming a daily deposition of growth increments, the results indicate that the increments on the beak of *S. esculenta* are clearly defined and suitable for age determination. The estimated ages ranged from 59 to 152 days, with minimal differences observed between male and female individuals. The *S. esculenta* specimens were relatively young and exhibited low sexual maturity, indicating that the growth model primarily reflects the early developmental stages. The growth relationship between age and ML is best represented by a linear model, whereas the relationship between age and BW follows different growth patterns: females conform to an exponential model, and males follow a power function model. Growth rate analysis demonstrates that both ML and BW exhibit varying growth rates at different age stages, with the highest growth rates observed at 120–150 days and 60–90 days, respectively, this may reflect different energy allocations at distinct growth stages. This study offers preliminary insights into the biological characteristics of the *S. esculenta* population in the East coast of China and offers scientific evidence for fishery resource management, sustainable population utilization, and ecological conservation. Future research should continue to focus on the spatiotemporal variability of *S. esculenta*, conducting long-term sampling programs to further refine its age-growth model and assess trends in resource changes.

Data availability statement

The raw data supporting the conclusions of this article will be made available by the authors, without undue reservation.

Ethics statement

The manuscript presents research on animals that do not require ethical approval for their study.

Author contributions

BLL: Visualization, Project administration, Resources, Validation, Writing – review & editing, Conceptualization. YZO: Writing – original draft, Methodology, Software, Data curation, Investigation, Formal analysis. MHZ: Writing – review & editing, Validation, Investigation, Software. HZ: Investigation, Writing – review & editing, Project administration. YYX: Writing – review & editing, Conceptualization. KWZ: Investigation, Writing – original draft. CWZ: Visualization, Writing – original draft. HSH: Investigation, Writing – original draft.

Funding

The author(s) declare that financial support was received for the research and/or publication of this article. This research was supported by 2022 Jiangsu Provincial Agricultural Ecological Protection and Resource Utilization Special Fund -Fisheries Ecology and Resource Monitoring (2022-SJ-061-01), and 2021 Jiangsu Provincial Agricultural Ecological Protection and Resource Utilization Special Fund -Fisheries Ecology and Resource Monitoring (2021-SJ-110-02).

Acknowledgments

We would like to thank Jiangsu Marine Fisheries Research Institute for their support. Thanks to 2022 Annual Jiangsu Province Agricultural Ecological Protection and Resource Utilization Special Project - Fishery Ecology and Resource Monitoring (2022-SJ-061-01) and Annual Jiangsu Province Agricultural Ecological Protection and Resource Utilization Special Project - Fishery Ecology and Resource Monitoring (2021-SJ-110-02) for the partial support. Finally, we thank the editor and the reviewers whose comments greatly improved the manuscript.

Conflict of interest

The authors declare that the research was conducted in the absence of any commercial or financial relationships that could be construed as a potential conflict of interest.

Generative AI statement

The author(s) declare that no Generative AI was used in the creation of this manuscript.

Publisher's note

References

Agus, B., Ruiu, S., Cera, J., Bellodi, A., Pasquini, V., and Cuccu, D. (2024). Age estimation in sepia officinalis using beaks and statoliths. *Animals* 14, 2230. doi: 10.3390/ani14152230

Al-Rawe, R. A., Al-Rammahi, H. M., Cahyanto, A., Ma'amor, A., Liew, Y. M., Sukumaran, P., et al. (2024). Cuttlefish-bone-derived biomaterials in regenerative medicine, dentistry, and tissue engineering: A systematic review. *J. Funct. Biomater.* 15, 219. doi: 10.3390/jfb15080219

Arkhipkin, A. I. (1997). Age of the micronektonic squid *Pterygioteuthis gemmata* (Cephalopoda: Pyroteuthidae) from the central-east Atlantic based on statolith growth increments. *J. Molluscan Stud.* 2), 287–290. doi: 10.1093/mollus/63.2.287

Arkhipkin, A. I. (2005). Statoliths as 'black boxes'(life recorders) in squid. *Mar. Freshw. Res.* 56, 573–583. doi: 10.1071/MF04158

Arkhipkin, A. I., and Laptikhovsky, V. V. (2000). Age and growth of the squid *Todaropsis eblanae* (Cephalopoda: Ommastrephidae) on the north-west African shelf. *J. Mar. Biol. Assoc. UK* 80, 747–748. doi: 10.1017/S0025315400002642

Armelloni, N. E., Lago-Rouco, J. M., Bartolomé, A., Felipe, B. C., and Perales-Raya, C. (2020). Exploring the embryonic development of upper beak in *Octopus vulgaris* Cuvier 1797: New findings and implications for age estimation. *Fish. Res.* 221, 105375. doi: 10.1016/j.fishres.2019.105375

Boyle, P., and Rodhouse, P. (2005). *Cephalopods: Ecology and Fisheries* (Oxford: Blackwell), ISBN: .

Boyle, P., and Rodhouse, P. (2008). *Cephalopods: Ecology and Fisheries* (Hoboken, New Jersey, USA: John Wiley & Sons).

Brunetti, N. E., and Ivanovic, M. L. (1997). Description of *Illex argentinus* beaks and rostral length relationsillps with size and weight of squids. *Rev. Investig. Desarro. Pesq. (Buenos Aires).* 11 (2), 7–18. Available online at: https://expydoc.com/doc/50804/rev-invest-desarr-pesq-11-135-144.pdf

Castanhari, G., and Tomás, A. R. G. (2012). Beak Increment conts as a tool for growth studies of the common octopus, *Octopus vulgaris*, in southern Brazil. *Bol Inst Pesca* 38, 323–331. doi: 10.3897/zookeys.245.3416

Chen, X., Han, F., Zhu, K., Punt, A. E., and Lin, D. (2020). The breeding strategy of female jumbo squid *Dosidicus gigas*: energy acquisition and allocation. *Sci. Rep.* 10, 9639. doi: 10.1038/s41598-020-66703-5

Chen, X., Li, J., Liu, B., Chen, Y., Li, G., Fang, Z., et al. (2013). Age, growth and population structure of jumbo flying squid, *Dosidicus gigas*, off the Costa Rica Dome. *J. Mar. Biol. Assoc. UK* 93, 567–573. doi: 10.1017/S0025315412000422

Chen, X., Lu, H., Liu, B., Chen, Y., Li, G., Fang, Z., et al. (2011). Age, growth and population structure of jumbo flying squid, *Dosidicus gigas*, based on statolith microstructure off the Exclusive Economic Zone of Chilean waters. Marine Biological Association of the United Kingdom. *J. Mar. Biol. Assoc. UK* 91, 229–235. doi: 10.1017/S0025315410001438

Chen, Z., Lu, H., Liu, W., Liu, K., and Chen, X. (2022). Beak microstructure estimates of the age, growth, and population structure of purpleback flying squid (*Sthenoteuthis oualaniensis*) in the Xisha islands waters of the South China Sea. *Fishes* 7, 187–187. doi: 10.3390/FISHES7040187

Clarke, M. (1962). The identification of cephalopod "beaks" and the relationship between beak size and total body weight. *Bull. Br. Museum Natural History. Zool.* 8, 419–480. doi: 10.1016/0011-7471(64)90211-6

Clarke, M., Clarke, M. R., Clarke, M. W., Clarke, K. R., Clarke, K. R., and Clarke, M. (1986). A handbook for the identification of cephalopod beaks. *A Handb. Sheep Clinician* 10, 334–334. doi: 10.1186/ar2396

Cobb, C. S., Pope, S. K., and Williamson, R. (1995). Circadian rhythms to light-dark cycles in the lesser octopus, Eledone clrrhosa. *Mar. Freshw. Behav. Physiol.* 26 (1), 47–57. doi: 10.1080/10236249509378927

Dan, Y., Liu, B., Zou, L., Lu, J., and Song, L. (2025). Impact of water temperature experienced in early life of *Dosidicus gigas* on its adult growth. *Fish. Res.* 2025, 281107260–107260. doi: 10.1016/J.FISHRES.2024.107260

Dawe, E. G., and Beck, P. C. (1997). Population structure, growth, and sexual maturation of short-finned squid (*Illex illecebrosus*) at Newfoundland. *Can. J. Fish. Aquat.Sci.* 54, 137–146. doi: 10.1139/F96-263

Dong, Z. Z. (1991). *Biology of the Economic Species of Cephalopods in the World Oceans* (Jinan: Shandong Science & Technology Press), 197–207.

Fang, Z., Li, J., Thompson, K., Hu, F., Chen, X., Liu, B., et al. (2016). Age, growth, and population structure of the red flying squid (*Ommastrephes bartramii*) in the North Pacific Ocean, determined from beak microstructure. *Fish B-Noaa* 114, 34–44. doi: 10.7755/FB.114.1.3

Fang, Z., Yu, J., Yang, G., and Han, P. (2022). Microstructure of Beak and Cuttlebone and Determination of Growth Increments for *Sepia esculentas* off Coast of East China Sea. *J. Guangdong Ocean Univ.* 42, 46–52. doi: 10.3969/j.issn.1673-9159.2022.02.006

Fei, Y. (2020). Preliminary study on the growth characteristics of *Sepia esculenta* from the coastal waters of Lanshantou, Rizhao City. *J. Aquacult.* 41, 35–38. doi: 10.3969/j.issn.1004-2091.2020.03.008

Forsythe, J. W., and Van Heukelem, W. F. (1987). "Growth," in *Cephalopod Life Cycles Volume II*. Ed. P. R. Boyle (London: Academic Press), 135–156.

Guerra-Marrero, A., Aurora, B., Lorena, M. C., Ana, E. R., and David, A. J. (2023b). Age, growth, and population structure of the African cuttlefish *Sepia bertheloti* based on beak microstructure. *Mar. Biol.* 170(10), 118. doi: 10.1007/S00227-023-04272-7

Guerra-Marrero, A., Perales-Raya, C., Lishchenko, F., Espino-Ruano, A., Jiménez-Alvarado, D., Couce-Montero, L., et al. (2023a). Age validation in the early stages of *Sepia officinalis* from beak microstructure. *Mar. Biol.* 170, 24. doi: 10.1007/s00227-022-04165-1

Guo, H. Y., Zhang, D. X., Näslund, J., Wang, L., and Zhang, X. (2022). Effects of spawning group sex ratio and stocking density on the outcome of captive reproduction in golden cuttlefish *Sepia esculenta*. *Aquaculture* 559. doi: 10.1016/J.AQUACULTURE.2022.738416

Guo, Y., Zeng, X., Wu, W., Ling, W., Zhao, C., Li, Y., et al. (2023). Age and growth of *Sthenoteuthis oualaniensis* based on statolith in the Eastern Indian Ocean. *J. Fish. China* 45, 887–898.

Hao, Z., Zhang, X., and Zhang, P. (2007). Biological characteristics and multiplication techniques of *Sepia esculenta*. *Chin. J. Ecol.* 04), 601–606. doi: 10.13292/j.1000-4890.2007.010

Harvey, T. J., Friend, T., and McHuron, A. E. (2014). Cephalopod remains from stomachs of sperm whales (Physeter macrocephalus) that mass-stranded along the Oregon coast. *Mar. Mamm. Sci.* 30, 609–625. doi: 10.1111/mms.12063

Hernández-López, J. L., Castro-Hernández, J. J., and Hernández-García, V. (2001). Age determined from the daily deposition of concentric rings on common octopus (*Octopus vulgaris*) beaks. *Fish B-Noaa* 99, 679–684. doi: 10.1046/j.1444-2906.2001.00353.x

Hu, G., Fang, Z., Liu, B., Yang, D., Chen, X., and Chen, Y. (2016). Age, growth and population structure of jumbo flying squid *Dosidicus gigas* off the Peruvian Exclusive Economic Zone based on beak microstructure. *Fish. Sci.* 82, 597–604. doi: 10.1007/s12562-016-0991-y

Ikeda, Y., Ueta, Y., Anderson, F. E., and Matsumoto, G. (2009). Reproduction and life span of the oval squid *Sepioteuthis lessoniana* (Cephalopoda: Loliginidae): comparison between laboratory-cultured and wild-caught squid. *Mar. Biodiversity Records* 2, e50. doi: 10.1017/S175526720900061X

Jackson, G. D. (2004). Advances in defining the life histories of myopsid squid. *Mar. Freshw. Res.* 55, 357–365. doi: 10.1071/MF03152

Jahan, R., and Mahmud, N. M. (2025). Length-weight relationship, condition factors and reproductive biology of the spineless cuttlefish *Sepiella inermis* (Ferussac & d'Orbigny 1848) in the southeastern regions of the Bay of Bengal, Bangladesh. *Heliyon* 11, e42338–e42338. doi: 10.1016/j.heliyon.2025.e42338

Li, N., Yu, J., Fang, Z., Chen, X., and Zhang, Z. (2021). Age, growth and population structure of swordtip squid (*Uroteuthis edulis*) in the East China Sea based on statolith age information. *J. Fish. China* 45, 887–898. doi: 10.11964/jfc.20200212154

Liu, L., Chen, X., Chen, Y., and Hu, G. (2015). Determination of squid age using upper beak rostrum sections: technique improvement and comparison with the statolith. *Mar. Biol.* 162, 1685–1693. doi: 10.1007/s00227-015-2702-0

Liu, B., Chen, X., and Yi, Q. (2013). A comparison of fishery biology of jumbo flying squid, *Dosidicus gigas* outside three Exclusive Economic Zones in the Eastern Pacific Ocean. *Chin. J. Oceanol. Limnol.* 31, 523–533. doi: 10.1007/s00343-013-2182-3

Liu, B., Lin, J., Chen, X., and Hu, G. (2016). Beak microstructure and validation of growth increments of neon flying squid in the northwest Pacific Ocean. *Oceanol. Limnol. Sin.* 4), 7. doi: 10.11693/hyhz20160300044

Liu, B., Liu, N., Li, J., and Zhang, X. (2020). Beak microstructure and its application in age and growth study of *Dosidicus gigas* in open sea of Chile. *South China Fish. Sci.* 16, 62–68. doi: 10.12131/20190116(

Lu, H. J., Ou, Y. Z., He, J. R., Zhao, M. L., Chen, Z. Y., and Chen, X. J. (2022). Age, growth and population structure analyses of the purpleback flying squid *Sthenoteuthis oualaniensis* in the northwest Indian Ocean by the statolith microstructure. *J. Mar. Sci. Eng.*, 10 (8), 1094.

Miserez, A., Li, Y., Waite, J. H., and Zok, F. (2007). Jumbo squid beaks: Inspiration for design of robust organic composites. *Acta Biomater.* 3, 139–149. doi: 10.1016/j.actbio.2006.09.004

Miserez, A., Weaver, J. C., Pedersen, P. B., Schneeberk, T., Hanlon, R. T., Kisailus, D., et al. (2010). Microstructural and biochemical characterization of the nanoporous sucker rings from *Dosidicus gigas*. *Adv. Mater.* 21, NA–NA. doi: 10.1002/adma.200990009

Natsukari, Y., and Tashiro, M. (1991). Neritic squid resources and cuttlefish resources in Japan. *Mar. Freshw. Behav. Physiol.* 18, 149–226. doi: 10.1080/10236249109378785

Niu, C., Yang, C., Huang, Y., and Zhang, X. (2017). The efficacy of new spawning substrates for *Sepia esculenta* oosperm adhesion. *J. Fish. Sci. China* 24, 11. doi: 10.3724/SP.J.1118.2017.16368

Oosthuizen, A. (2003). *A development and management framework for a new Octopus vulgaris fishery in South Africa* (PhD diss., Rhodes University), 203 pp.

Ou, Y., Lu, H., Wang, H., Chen, Z., and Zhao, M. (2022). Age, growth and population structure analyses of the purpleback flying squid *Sthenoteuthis oualaniensis* in the northwest Indian Ocean by the statolith microstructure. *Fishes* 7, 324–324. doi: 10.3390/FISHES7060324

Pascual, C., Cruz-Lopez, H., Mascaró, M., Gallardo, P., Sánchez, A., Domingues, P., et al. (2020). Changes in biochemical composition and energy reserves associated with sexual maturation of *Octopus maya*. *Front. Physiol.* 11. doi: 10.3389/fphys.2020.00022

Perales-Raya, C., Almansa, E., Bartolomé, A., Felipe, B. C., and Rodriguez, C. (2014a). Age validation in *Octopus vulgaris* beaks across the full ontogenetic range: beaks as recorders of life events in octopuses. *J. Shellfish Res.* 33, 481–493. doi: 10.2983/035.033.0217

Perales-Raya, C., Bartolomé, A., García-Santamaría, T. M., Pascual-Alayón, P., and Almansa, E. (2010). Age estimation obtained from analysis of octopus (*Octopus vulgaris* Cuvier 1797) beaks: Improvements and comparisons. *Fish. Res.* 106, 171–176. doi: 10.1016/j.fishres.2010.05.003

Perales-Raya, C., Bartolomé, A., Hernández-Rodríguez, E., Carrillo, M., Martín, V., and Fraile-Nuez, E. (2020). How old are giant squids? First approach to aging Architeuthis beaks. *Bull. Mar. Sci.* 96, 357–374. doi: 10.5343/bms.2019.0041

Perales-Raya, C., Fernandez-Nunez, M., Balguerías-Guerra, E., and Hernández-González, C. (1994). Progress toward ageing cuttlefish (*Sepia hierredda* Rang 1837) from northwest African coast using statoliths. *Mar. Ecol. Prog. Ser.* 114, 139–147. doi: 10.3354/MEPS114139

Perales-Raya, C., Jurado-Ruzafa, A., Bartolomé, A., Duque, V., Carrasco, M. N., and Fraile-Nuez, E. (2014b). Age of spent *Octopus vulgaris* and stress mark analysis using beaks of wild individuals. *Hydrobiologia* 725, 105–114. doi: 10.1007/s10750-013-1602-x

Qi, Z. Y. (1998). *Economic Mollusca of China* (Beijing: China Agriculture Press), 293–294.

Qu, J., Zhou, M., Han, P., and Chen, X. (2021). Age and growth characteristic of *Sepia officinalis* in the West Africa based on cuttlebones. *Chin. J. Appl. Ecol.* 32, 1873–1880. doi: 10.13287/j.1001-9332.202105.035

Raya, C. P., and Hernández-González, C. L. (1998). Growth lines within the beak microstructure of the octopus *Octopus vulgaris* Cuvier 1797. *Afr. J. Mar. Sci.* 20, 135–142. doi: 10.2989/025776198784126368

Sajikumar, K. K., Ragesh, N., Venkatesan, V., Koya, K. P., Sasikumar, G., Kripa, V., et al. (2018). Morphological development and distribution of paralarvae juveniles of purple back flying squid *Sthenoteuthis oualaniensis* (Ommastrephidae), in the south eastern Arabian Sea. *Sea. Vie et milieu-life and enVironment* 68 (2-3), 75-86.

Sieiro, P., Otero, J., and Aubourg, S. P. (2020). Biochemical composition and energy strategy along the reproductive cycle of female *Octopus vulgaris* in Galician waters (NW Spain). *Front. Physiol.* 11. doi: 10.3389/FPHYS.2020.00760

Wei, L., Gao, T., Han, Z., Liu, Z., and Wang, Z. (2005). Biology of *Sepia esculenta* from the coastal waters of Rizhao. *Period. Ocean Univ. China* 06), 45–50. doi: 10.16441/j.cnki.hdxb.2005.06.009

Xavier, J. C., Golikov, A. V., Queirós, J. P., Perales, R. C., Rosas, L. R., Abreu, J., et al. (2023). Corrigendum: The significance of cephalopod beaks as a research tool: An update. *Front. Physiol.* 75, 141140110–1140110. doi: 10.3389/FPHYS.2023.1140110

Xue, W., Xu, H., Guo, R., and Fang, Z. (2024). Characteristics of growth and gonadal development and estimation of first sexual maturity mantle length of *Sepia esculenta*. *J. Shanghai Ocean Univ.* 33, 715–727. doi: 10.12024/jsou.20230604255

Yatsu, A., Midorikawa, S., Shimada, T., and Uozumi, Y. (1997). Age and growth of the neon flying squid, *Ommastrephes bartrami*, in the North Pacific ocean. *Fish. Res.* 29 (3), 257–270. doi: 10.1016/S0165-7836(96)00541-3

Zhao, Z., Hu, G., Chen, L., Chen, Y., Guo, F., and Fang, Z. (2024). Ontogenetic, sexual, and monthly niche segregation of *Sepia esculenta* in the northern East China Sea revealed by stable carbon and nitrogen isotopes. *Mar. Biotechnol.* 26(5), 1–10. doi: 10.1007/S10126-024-10352-6